

## Kinetic Analyses of an Electrochemically-Induced Reaction through a Generation-Collection Mode of Twin-Microband Electrodes

Kiyoharu Nakatani,\* Norifumi Terui, and Noboru Kitamura\*

Division of Chemistry, Graduate School of Science, Hokkaido University, Kita-ku, Sapporo 060

(Received October 31, 1995)

Kinetic analyses of a sulfonation reaction between electrochemically-generated diethyl(4-imino-3-methyl-2,5-cyclohexylidene)ammonium salt (quinone diimine derivative (QDI) and  $\text{SO}_3^{2-}$  in water have been performed by a generation-collection mode of twin-microband electrodes. The collection efficiency of QDI ( $\phi$ ), defined as the ratio of the current at a generator to that at a collector, was dependent on the interelectrode distance and the  $\text{SO}_3^{2-}$  concentration. The rate constant of the sulfonation reaction was determined by both a two-dimensional digital simulation of the concentration gradient of QDI and kinetic analyses of the observed  $\phi$  values.

Kinetic analyses of homogeneous chemical reactions in solution have been conducted by a variety of electrochemical techniques.<sup>1)</sup> Among them, rotating ring-disk electrode and double-step chronocoulometric methods enable one successive generation and collection of redox species. When an electrochemically-generated species undergoes a reaction in solution, the relevant collection efficiency of the species ( $\phi$ ), defined as the ratio of the current for generation to that for collection, decreases, and, therefore, the kinetic parameters of the reaction can be determined through an observation of the  $\phi$  values under various conditions. Analogous studies can be made using a microelectrode array, in which band electrodes are spatially arranged in micrometer dimensions with well-defined geometries, such as the size of an electrode, the electrode-electrode distance ( $l$ ) and so forth.<sup>2–8)</sup> In a microelectrode array, since a redox species generated at one electrode should diffuse to another electrode for collection, the  $\phi$  value would be strongly influenced by reactions in the solution phase.<sup>3)</sup> As one of the advantages of an electrode array,  $l$  can be arbitrarily varied so that kinetic analyses of electrochemically-induced reactions can be conducted in an elaborate fashion through a study on the  $l$  dependence of the  $\phi$  value.

In order to reveal the characteristic features of chemical reactions in micrometer dimensions, we have focused our attention on studying the mass-transfer and electron-transfer processes across a single microdroplet/solution interface.<sup>9–11)</sup> By potential applications of a laser trapping-spectroscopy-electrochemistry technique, we actually previously reported on a dye-formation reaction between diethyl(4-imino-3-methyl-2,5-cyclohexylidene)ammonium salt (quinone diimine derivative (QDI)) generated by a microelectrode in water and a solute in a laser-manipulated oil droplet. We also demonstrated that the reaction efficiency is highly dependent on the droplet-microelectrode distance, since diffusion of QDI in water competed with sulfonation

and/or deamination reaction(s), as illustrated in Fig. 1a.<sup>10)</sup> Although microscopic mechanisms of the dye-formation reaction could be discussed in terms of the concentration gradient of QDI along the direction between the electrode and the droplet, the kinetic aspect of the contributions of the sulfonation/deamination reaction of QDI to dye formation was still ambiguous. If the microdroplet in Fig. 1a is replaced by a microelectrode in an analogous system, mass-transfer processes and the side-reaction(s) of QDI could be elucidated quantitatively through generation-collection experiments of QDI by microelectrodes (Fig. 1b). The experiments illustrated in Figs. 1a and 1b are complementary, and an inside look at the dye-formation reaction will be obtained by both approaches.

In this article we report on kinetic analyses of the mass transfer and a sulfonation reaction of QDI on the basis of a generation-collection mode of a pair of microelectrodes: twin-microband electrode. The rate constant of the sulfonation reaction was determined by analyzing the electrode-electrode distance dependence of the collection efficiency of QDI, and compared with that estimated by a digital simulation of the QDI diffusion.

### Experimental

*N,N*-Diethyl-4-amino-3-methylaniline (*p*-phenylenediamine derivative (PPD), Kodak) was recrystallized from ethanol in the presence of *p*-toluene sulfonic acid.  $\text{Na}_2\text{SO}_3$  (Wako Pure Chemicals) was recrystallized from water. Water was purified by distillation and deionization (GSR-200, Advantec Toyo). All other chemicals were used without further purification. As a sample solution, PPD ( $1.0 \text{ mmol dm}^{-3}$ ) and an appropriate amount of  $\text{Na}_2\text{SO}_3$  ( $1.0$ – $5.0 \text{ mmol dm}^{-3}$ ) were dissolved in a  $\text{K}_2\text{CO}_3$  ( $0.4 \text{ mol dm}^{-3}$ )/ $\text{KHCO}_3$  ( $0.32 \text{ mol dm}^{-3}$ ) buffer solution (pH=10) containing KCl ( $0.1 \text{ mol dm}^{-3}$ ).

Gold twin-microband working electrodes ( $60.0 \mu\text{m}$  length  $\times$   $10.0 \mu\text{m}$  width  $\times$   $0.3 \mu\text{m}$  thickness for each electrode) with an electrode-electrode distance ( $l$ ) of 2.0, 5.0, or  $10.0 \mu\text{m}$  and a gold counter

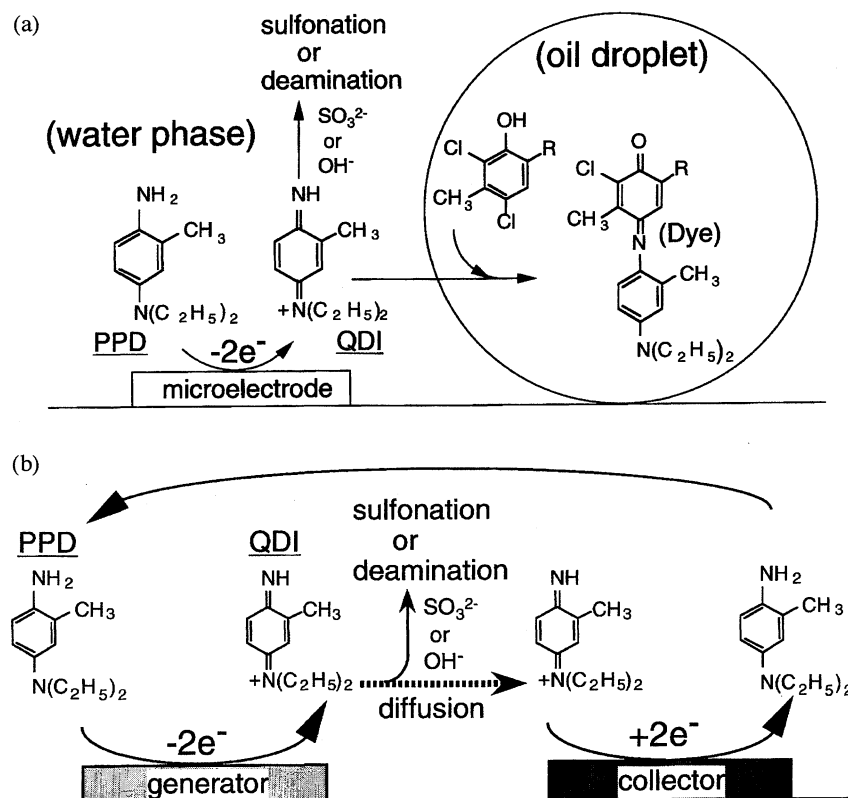


Fig. 1. General schemes of electrochemically-induced reactions of QDI in the droplet/microelectrode (a) and twin-electrodes (b) systems.

electrode (3.5 mm length  $\times$  0.2 mm width  $\times$  0.3  $\mu\text{m}$  thickness) were fabricated on a Si wafer by photolithography. Ag/AgCl(NaCl(sat.)) was used as a reference electrode. Electrochemical responses were measured by a dual potentiostat system (BS-1, BAS). All measurements were performed under an  $\text{N}_2$  atmosphere at room temperature (ca. 23  $^\circ\text{C}$ ).

## Results and Discussion

### Electrochemical Measurements and Digital Simulations of the Rate of the Sulfonation Reaction.

The kinetics of homogeneous chemical reactions in solution can be directly studied by using a pair of microelectrodes (twin-electrodes) through the generation and collection of a redox species. In the present case (Fig. 1b), two-electron oxidation of PPD at one working electrode (generator electrode; GE) produces QDI, and QDI can be successively reduced to PPD at another electrode (collector electrode; CE) spaced several micrometers from GE, if an appropriate potential is applied to each electrode. During the diffusion of QDI in the solution phase, on the other hand, QDI undergoes sulfonation and deamination reactions with  $\text{SO}_3^{2-}$  and  $\text{OH}^-$ , respectively, so that the regeneration of PPD at CE competes with these side reactions. However, the rate constants of the deamination and sulfonation reactions of QDI have been reported to be ca. 0.2  $\text{s}^{-1}$  and ca.  $10^4 \text{ mol}^{-1} \text{ dm}^3 \text{ s}^{-1}$  at pH=10, respectively,<sup>12,13</sup> so that sulfonation of QDI would be the major reaction path under the present condition of  $[\text{SO}_3^{2-}] = 1.0\text{--}5.0 \text{ mmol dm}^{-3}$ . Furthermore, the diffusion length of QDI is very short, due to the small gap width be-

tween the two electrodes ( $<10 \mu\text{m}$ ). This also suggests that the deamination reaction can be neglected as a side reaction of QDI. When one observes the currents at GE ( $i_g$ ) and CE ( $i_c$ ), therefore, the collection efficiency of QDI, defined as  $\phi = i_c/i_g$ , can be used as a measure of the contribution of the sulfonation reaction to the fate of QDI.

Figure 2 shows cyclic voltammograms of a PPD/QDI couple observed at GE and CE in the absence of  $\text{SO}_3^{2-}$ , where the potential of GE is swept between  $-0.1$  and  $+0.15 \text{ V}$  (vs. Ag/AgCl), while that at CE is fixed at  $-0.1 \text{ V}$  ( $l = 2 \mu\text{m}$ ). The current-potential curves were sigmoidal at a potential sweep rate of  $10 \text{ mV s}^{-1}$ , characteristic to an electrochemical response of a microelectrode. Knowing that a two-electron oxidation potential of PPD to QDI is ca. 30 mV at pH=10,<sup>10,11</sup> we conclude that the anodic ( $i_g$ ) and cathodic currents ( $i_c$ ) correspond to the oxidation of PPD and the reduction of QDI, respectively. When  $l$  was varied from 2 to 5 or 10  $\mu\text{m}$  ( $[\text{SO}_3^{2-}] = 0$ ), the  $\phi$  value decreased from 0.51 to 0.24 along with an increase in  $l$ , as shown in Fig. 3. The decreasing order of  $\phi$  with  $l$  agreed very well with the  $l$  dependence of  $\phi$  for a  $\text{Ru}(\text{NH}_3)_6^{3+}/\text{Ru}(\text{NH}_3)_6^{2+}$  couple in water (determined by a separate experiment). These results indicate that a contribution of the deamination reaction of QDI to  $\phi$  is negligible, as expected from above discussion.

In the presence of  $\text{SO}_3^{2-}$ , analogous cyclic voltammograms with those in Fig. 2 were observed. However, the current at CE was strongly dependent on the concentration of  $\text{SO}_3^{2-}$  and decreased with increasing  $[\text{SO}_3^{2-}]$ , indicating the reaction of QDI with  $\text{SO}_3^{2-}$  in the water phase. Further-

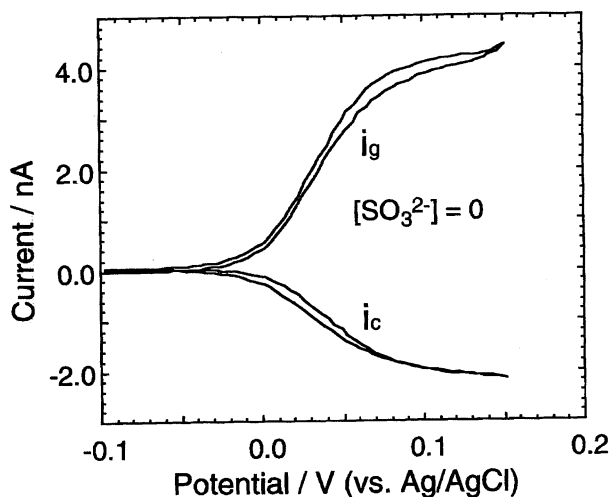


Fig. 2. Cyclic voltammograms of a PPD/QDI couple observed at GE and CE ( $l = 2.0 \mu\text{m}$ ,  $[\text{PPD}] = 1.0 \text{ mmol dm}^{-3}$  and  $[\text{SO}_3^{2-}] = 0$ ). The potential at GE was swept between  $-0.1$  and  $+0.15 \text{ V}$  (vs. Ag/AgCl,  $10 \text{ mV s}^{-1}$ ) while that at CE was set  $-0.1 \text{ V}$ .

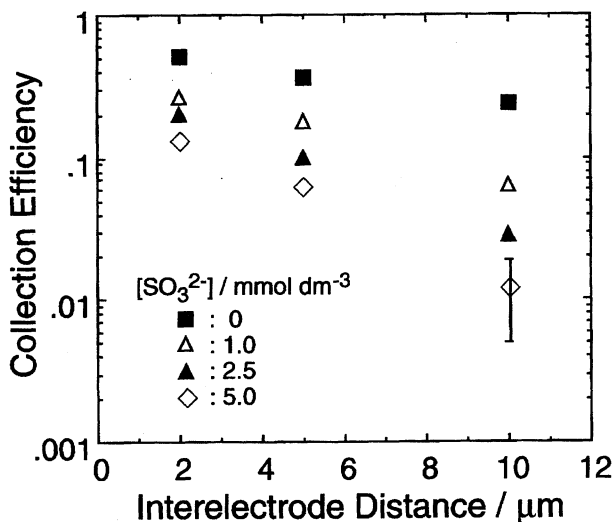


Fig. 3. Interelectrode distance ( $l$ ) dependencies of the collection efficiency.  $[\text{SO}_3^{2-}] = 0$  (■),  $1.0$  (△),  $2.5$  (▲), and  $5.0 \text{ mmol dm}^{-3}$  (◇). See also Ref. 14.

more,  $i_g$  was slightly smaller than that in Fig. 2 owing to a decrease in the amount of reproduced PPD at CE by the sulfonation reaction (i.e., feedback current by redox cycling). In total, the  $\phi$  value decreased along with an increase in  $[\text{SO}_3^{2-}]$ . The  $\phi$  value was also dependent on  $l$ , as shown in Fig. 3.<sup>14</sup> The data given in Fig. 3 explicitly demonstrate that QDI produced at GE reacts with  $\text{SO}_3^{2-}$  in competition with diffusion to CE. The kinetics of the sulfonation reaction can be analyzed on the basis of the  $l$  and  $[\text{SO}_3^{2-}]$  dependencies of the  $\phi$  value.

One possible approach to analyze the  $l$  dependence of  $\phi$  is a two-dimensional ( $X$ - $Y$  plane) digital simulation of the diffusion of PPD and QDI in the water phase, since a methodology has been reported by Bard et al.<sup>2,3</sup> When the sulfonation reaction of QDI (rate constant;  $k_s$ ) is taken into

account, the time dependencies of the concentrations of PPD, QDI, and  $\text{SO}_3^{2-}$  in the  $X$ - $Y$  plane are given as in the following Eqs. 1, 2, and 3, respectively:

$$\frac{\partial[\text{PPD}]}{\partial t} = D_P[(\partial^2[\text{PPD}]/\partial x^2) + (\partial^2[\text{PPD}]/\partial y^2)], \quad (1)$$

$$\frac{\partial[\text{QDI}]}{\partial t} = D_Q[(\partial^2[\text{QDI}]/\partial x^2) + (\partial^2[\text{QDI}]/\partial y^2)] - k_s[\text{QDI}][\text{SO}_3^{2-}]t, \quad (2)$$

$$\frac{\partial[\text{SO}_3^{2-}]}{\partial t} = D_S[(\partial^2[\text{SO}_3^{2-}]/\partial x^2) + (\partial^2[\text{SO}_3^{2-}]/\partial y^2)] - k_s[\text{QDI}][\text{SO}_3^{2-}]t, \quad (3)$$

where  $D_P$ ,  $D_Q$ , and  $D_S$  are the diffusion coefficients of PPD, QDI, and  $\text{SO}_3^{2-}$  in water, respectively, which are assumed to be equal to that of PPD ( $5 \times 10^{-6} \text{ cm}^2 \text{ s}^{-1}$  as determined by cyclic voltammetry). The sulfonation reaction proceeds via a second-order kinetics, as expressed as the third term of the right-hand side of Eqs. 2 and 3. In a two-dimensional simulation the diffusion of PPD, QDI, or  $\text{SO}_3^{2-}$  was approximated to proceed hemi-cylindrically in the  $X$ - $Y$  plane along the length of the working electrode ( $Z$  axis;  $60 \mu\text{m}$ ). Equations 1, 2, and 3 can be solved numerically by a finite-differential model under the conditions of  $\Delta x = \Delta y = 1 \mu\text{m}$  and  $\Delta t = 4.8 \times 10^{-4} \text{ s}$  (i.e.;  $D\Delta t/\Delta x^2 = D\Delta t/\Delta y^2 = 0.24$ ). The  $\phi$  value should be equal to the ratio of  $[\text{QDI}]$  at GE to that at CE, so that  $\phi$  can be simulated by Eqs. 1, 2, and 3 with various  $k_s$  values (the results are summarized in Fig. 4).

At  $[\text{SO}_3^{2-}] = 0$  (i.e.,  $k_s = 0$ ), the simulated  $\phi$  values were somewhat larger than the experimental data, and the deviation between two values increased with increasing  $l$ . It is noteworthy that this is not unusual for the present simulation model, and that analogous results have been reported by Bard et al. as well.<sup>2)</sup> In the model, the length of GE is assumed to be infinite compared with  $l$ . In actual experiments, on the other hand, the electrode length ( $60 \mu\text{m}$ ) is not

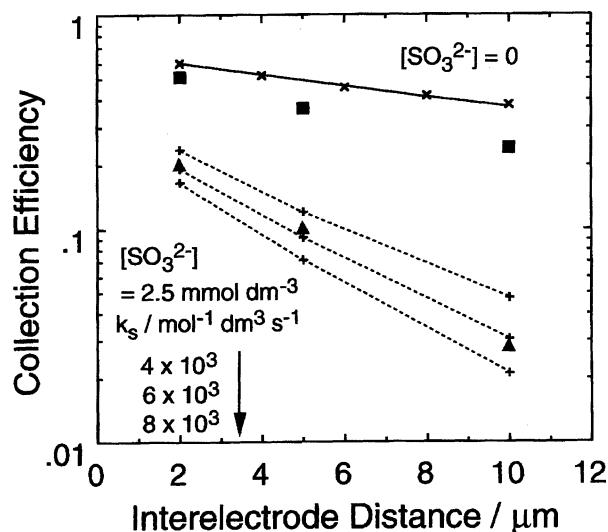


Fig. 4. Interelectrode distance dependencies of the collection efficiency.  $[\text{SO}_3^{2-}] = 0$  (■) and  $2.5 \text{ mmol dm}^{-3}$  (▲). The solid and broken curves represent the simulated ones for the data at  $[\text{SO}_3^{2-}] = 0$  and  $2.5 \text{ mmol dm}^{-3}$ , respectively.

long enough relative to  $l$  ( $=2\text{--}10\text{ }\mu\text{m}$ ), so that QDI escapes from GE toward the Z direction to some extent. The escape yield increases with increasing  $l$ , rendering a relatively large deviation at larger  $l$ . This leads to a decrease in  $i_c$  so that the observed  $\phi$  values are smaller than the simulated values. As judged from the observed and simulated values, we conclude that the simulation overestimates  $\phi$  by 15–20%.

A simulation was also performed for the data in the presence of  $\text{SO}_3^{2-}$ ; as a typical example,  $[\text{SO}_3^{2-}] = 2.5\text{ mmol dm}^{-3}$  is included in Fig. 4. Although the observed data were simulated by  $k_s = (4\text{--}8) \times 10^3\text{ mol}^{-1}\text{ dm}^3\text{ s}^{-1}$ , the best fit was obtained with  $k_s = 6 \times 10^3\text{ mol}^{-1}\text{ dm}^3\text{ s}^{-1}$ . Similarly, the data at  $[\text{SO}_3^{2-}] = 1.0$  and  $5.0\text{ mmol dm}^{-3}$  were also well reproduced with the common  $k_s$  value. By taking the error in determining  $\phi$  by a simulation (15–20%) into account,  $k_s$  was then determined to be  $(5\text{--}6) \times 10^3\text{ mol}^{-1}\text{ dm}^3\text{ s}^{-1}$ . The  $k_s$  value is comparable to that determined by a rotating ring-disk electrode ( $1 \times 10^4\text{ mol}^{-1}\text{ dm}^3\text{ s}^{-1}$ ; [PPD] =  $1.0\text{ mmol dm}^{-3}$  and  $[\text{SO}_3^{2-}] = 1.0\text{ mmol dm}^{-3}$ ) as well as to the reported value (ca.  $10^4\text{ mol}^{-1}\text{ dm}^3\text{ s}^{-1}$ ).<sup>13</sup> The sulfonation reaction of QDI in the water phase can be reasonably analyzed by generation-collection experiments and a digital simulation.

**Kinetic Determination of the Rate of the Sulfonation Reaction.** Besides the digital simulation, the  $k_s$  value can be directly determined by kinetic analyses of the  $l$  dependencies of  $\phi$  at various  $[\text{SO}_3^{2-}]$ , since the results involve information concerning the time dependence of QDI diffusion. The analyses were performed as follows. The rate of the sulfonation reaction is by

$$-d[\text{QDI}]/dt = k_s[\text{SO}_3^{2-}][\text{QDI}] \quad (4)$$

Under the condition  $[\text{SO}_3^{2-}] \gg [\text{QDI}]$  (discussed later), Eq. 4 was solved as a pseudo-first-order reaction,

$$\ln ([\text{QDI}]/[\text{QDI}]_0) = -k_s[\text{SO}_3^{2-}]t, \quad (5)$$

where  $[\text{QDI}]_0$  is the concentration of QDI at  $t=0$ , which is proportional to  $i_g$  at GE just after electrolysis. The diffusion time ( $t_{\text{cal}}$ ) of QDI from GE to CE was assumed to be equal to that from the center of GE to the neighboring edge of CE (distance =  $d$ ) and, could be calculated using  $t_{\text{cal}} = d^2/2D_{\text{Q}}$ . The concentration gradient of QDI along the direction from GE to the surrounding solution phase is considered to be independent of time at the steady state of current-potential curve measurements, owing to the spherical or cylindrical diffusion of QDI. Therefore,  $[\text{QDI}]/[\text{QDI}]_0$  at  $d$  should be proportional to  $\phi/\phi_0$ , where  $\phi_0$  is  $\phi$  at  $[\text{SO}_3^{2-}] = 0$  and constant at given  $d$ . Equation 5 is thus rewritten as

$$\ln \phi/\phi_0 = -k_s[\text{SO}_3^{2-}]t_{\text{cal}}, \quad (6)$$

which demonstrates a linear relationship between  $\ln(\phi/\phi_0)$  and  $[\text{SO}_3^{2-}]$  or  $t_{\text{cal}}$ . Actually, the  $\ln(\phi/\phi_0)$  value decreased linearly with an increase in  $[\text{SO}_3^{2-}]$  or  $t_{\text{cal}}$ , as shown in Figs. 5 and 6, respectively, indicating that the pseudo-first-order analyses were valid in the present system. The  $k_s$  value was thus determined to be  $(3\text{--}6) \times 10^3\text{ mol}^{-1}\text{ dm}^3\text{ s}^{-1}$  from

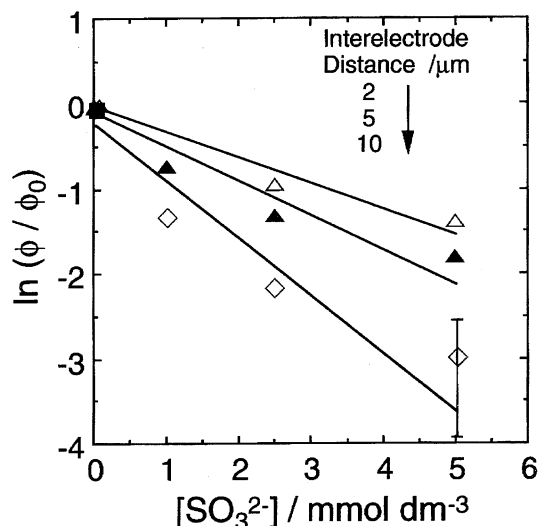


Fig. 5. Relationships between  $\ln(\phi/\phi_0)$  and  $[\text{SO}_3^{2-}]$  at  $l = 2.0, 5.0$ , and  $10.0\text{ }\mu\text{m}$ . See also Ref. 14.

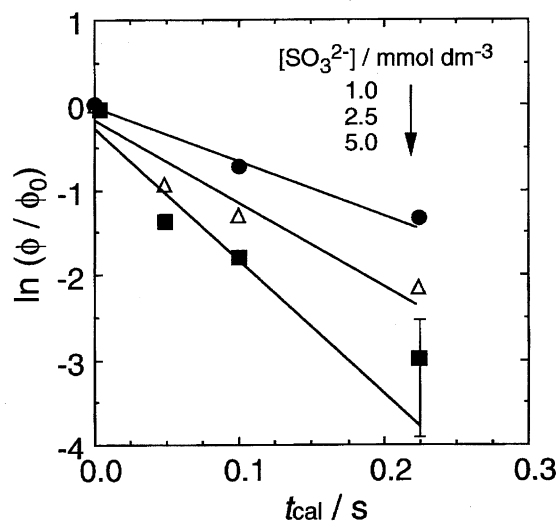


Fig. 6. Relationships between  $\ln(\phi/\phi_0)$  and  $t_{\text{cal}}$  at  $[\text{SO}_3^{2-}] = 1.0, 2.5$ , and  $5.0\text{ mmol dm}^{-3}$ . See also Ref. 14.

the slope of each plot in Figs. 5 and 6. It is noteworthy that  $\text{SO}_3^{2-}$  is consumed by the sulfonation reaction, so that the assumption that  $[\text{SO}_3^{2-}] \gg [\text{QDI}]$  ( $=1.0\text{ mmol dm}^{-3}$ ) may not necessarily be warranted, particularly at  $[\text{SO}_3^{2-}] = 1.0$  and  $2.5\text{ mmol dm}^{-3}$ . Nevertheless, even if  $\text{SO}_3^{2-}$  is consumed by the sulfonation reaction,  $\text{SO}_3^{2-}$  will be efficiently supplied from the bulk solution phase, since mass transfer from the bulk solution phase to the vicinity of the electrode is very fast, due to spherical diffusion. Therefore,  $[\text{SO}_3^{2-}]$  near the electrode will be approximated to be the same as the initial concentration, and the pseudo-first-order analyses can be applied to the results given in Figs. 5 and 6.

The experimentally determined  $k_s$  value agrees well with that calculated by a digital simulation ( $(5\text{--}6) \times 10^3\text{ mol}^{-1}\text{ dm}^3\text{ s}^{-1}$ ), and is also in good accordance with that determined by the dye-formation reaction in Fig. 1a (ca.  $5 \times 10^3\text{ mol}^{-1}\text{ dm}^3\text{ s}^{-1}$ ).<sup>10</sup> Since three different methods give a common  $k_s$  value, the present approaches are concluded to

be sufficiently powerful to study the kinetics of the chemical reactions in solution. In particular, the generation-collection of a redox species by a pair of microelectrodes and kinetic analyses of the relevant  $\phi$  values are very convenient and advantageous for studying both the mass transfer and subsequent chemical reactions in minute volumes.

### Conclusions

The sulfonation reaction between QDI and  $\text{SO}_3^{2-}$  in water was successfully analyzed on the basis of generation-collection experiments of QDI by twin-microband electrodes, and the rate constant was determined by both a digital simulation and the kinetic method. Thus, the microscopic mechanism and factors governing the dye-formation reaction in Fig. 1a are now clarified. According to the present results, the dye-formation reaction in a single oil droplet can be controlled by both the concentration of  $\text{SO}_3^{2-}$  in the water phase and the distance between GE and the droplet, depending on the rate and efficiency of the sulfonation reaction of QDI. We expect that the microscopic mechanisms of various chemical reactions in emulsion systems will be elucidated by potential applications of microchemical methods, such as microelectrode arrays, microspectroscopy, and laser trapping.

The authors are indebted to Prof. K. Hasebe, Graduate School of Environmental Earth Science, Hokkaido University, for generously allowing the use a rotating ring-disk electrode. The work was partly supported by a Grant-in-Aid on Priority-Area-Research "Photoreaction Dynamics" No. 07228203 from the Ministry of Education, Science and Culture, and the Toray Science Foundation.

### References

- 1) A. J. Bard and L. R. Faulkner, "Electrochemical Methods; Fundamentals and Applications," Wiley, New York (1980).
- 2) A. J. Bard, J. A. Crayston, G. P. Kittlesen, T. V. Shea, and M. S. Wrighton, *Anal. Chem.*, **58**, 2321 (1986).
- 3) T. V. Shea and A. J. Bard, *Anal. Chem.*, **59**, 2101 (1987).
- 4) K. Aoki, M. Morita, O. Niwa, and H. Tabei, *J. Electroanal. Chem.*, **256**, 269 (1986).
- 5) O. Niwa, M. Morita, and H. Tabei, *Anal. Chem.*, **62**, 447 (1990).
- 6) A. Aoki, T. Matsue, and I. Uchida, *Anal. Chem.*, **62**, 2206 (1990).
- 7) D. G. Sanderson and L. B. Anderson, *Anal. Chem.*, **57**, 2388 (1985).
- 8) C. E. Chidsey, B. J. Feldman, C. Lundgren, and R. W. Murray, *Anal. Chem.*, **58**, 601 (1986).
- 9) K. Nakatani, T. Uchida, and N. Kitamura, "Microchemistry; Spectroscopy and Chemistry in Small Domains," ed by H. Masuhara, F. C. DeSchryver, N. Kitamura, and N. Tamai, North-Holland, Amsterdam (1994), p. 549.
- 10) K. Nakatani, T. Suto, M. Wakabayashi, H.-B. Kim, and N. Kitamura, *J. Phys. Chem.*, **99**, 4745 (1995).
- 11) K. Nakatani, K. Chikama, H.-B. Kim, and N. Kitamura, *Chem. Phys. Lett.*, **237**, 133 (1995).
- 12) T. H. James, "The Theory of the Photographic Process," Macmillan, New York (1977).
- 13) S. Patai and Z. Rappoport, "The Chemistry of Quinoid Compounds," John Wiley & Sons, New York (1988).
- 14) At  $[\text{SO}_3^{2-}] = 5.0 \text{ mmol dm}^{-3}$ , the  $S/N$  values of the voltammograms observed at the twin-electrodes with  $l = 10 \text{ }\mu\text{m}$  were low because of low limiting currents (ca. 50 pA). An error in determining  $\phi$  was thus large as compared as those for other data points.